Supplemental Materials

Alteration of chain-length selectivity and thermostability of *Rhizopus oryzae* lipase via virtual saturation mutagenesis coupled with disulfide bond design

Jinsha Huang, Shuhan Dai, Xiying Chen, Li Xu*, Jinyong Yan, Min Yang, Yunjun Yan*

Key Laboratory of Molecular Biophysics, Ministry of Education, College of Life Science and Technology, Huazhong University of Science and Technology, Wuhan, People's Republic of China

*Corresponding authors:

Li Xu, xuli@hust.edu.cn; Yunjun Yan, yanyunjun@hust.edu.cn;

Table of Contents

bonds were as sticks in magenta.

Fig. S4 SDS-PAGE image of disulfide bond mutants using 12% separation gel and 5% stacking gel. (M: marker; 1: WT; 2: E265V/S267W; 3: E265V/S267W/E190C-E238C; 4: E265V/S267W/S61C-S115C; 5: M6).

Fig. S5 2D diagrams of enzyme–substrate interactions of five bound ligands generated by LigPlot+, and plot of variant E265V/S267W automatically fitted to WT. The ligands are: C8, C10, C12, C14, and C16.

Table S1 Binding/folding free energy changes of ROL variants predicted by Cartesian_ddg with a virtual scan

Mutation	Binding free energy change (kcal/mol)[a]					Folding free energy change (kcal/mol)[a]
	C8	C10	C12	C14	C16	Thermostability
P178C	–0.1 ± 0.0	–0.8 ± 0.0	0.0 ± 0.0	–0.4 ± 0.0	–0.2 ± 0.0	5.5 ± 0.0
P178L	–0.3 ± 0.0	–0.8 ± 0.0	–0.1 ± 0.0	–1.2 ± 0.0	–0.4 ± 0.0	3.2 ± 0.0
P178T	–0.2 ± 0.0	–0.7 ± 0.0	–0.2 ± 0.0	–0.3 ± 0.0	–0.1 ± 0.0	5.0 ± 0.0
P211C	0.0 ± 0.0	0.0 ± 0.0	–0.2 ± 0.0	–1.1 ± 0.0	–1.1 ± 0.1	5.3 ± 0.0
P211F	–0.2 ± 0.0	–0.3 ± 0.0	–0.4 ± 0.0	–3.7 ± 0.0	–1.5 ± 0.0	1.0 ± 0.0
P211H	–0.1 ± 0.0	–0.1 ± 0.0	–0.2 ± 0.0	–0.4 ± 0.0	–0.3 ± 0.0	1.6 ± 0.0
P211I	0.0 ± 0.0	0.0 ± 0.0	0.0 ± 0.0	–1.6 ± 0.0	–1.3 ± 0.0	5.5 ± 0.0
P211K	0.0 ± 0.0	0.0 ± 0.0	–0.1 ± 0.0	–0.3 ± 0.0	–0.2 ± 0.0	3.4 ± 0.0
P211L	0.0 ± 0.0	0.0 ± 0.0	–0.2 ± 0.0	–1.3 ± 0.0	–2.6 ± 0.5	2.4 ± 0.0
P211M	–0.1 ± 0.0	–0.1 ± 0.0	–0.1 ± 0.0	–1.2 ± 0.0	–1.8 ± 0.0	3.3 ± 0.0
P211Q	–0.1 ± 0.0	–0.1 ± 0.0	–0.2 ± 0.0	–0.8 ± 0.0	–1.2 ± 0.0	3.6 ± 0.0
P211R	–0.1 ± 0.0	–0.1 ± 0.0	–0.1 ± 0.0	–0.6 ± 0.0	–0.6 ± 0.0	4.2 ± 0.0
P211W	**–0.2 ± 0.0**	**–0.3 ± 0.0**	**–0.3 ± 0.0**	**–3.2 ± 0.0**	**–2.3 ± 0.0**	**–0.6 ± 0.0**
P211Y	–0.2 ± 0.0	–0.3 ± 0.0	–0.4 ± 0.0	–3.2 ± 0.0	–1.8 ± 0.0	0.5 ± 0.0
I254L	–0.4 ± 0.0	–0.9 ± 0.0	–1.1 ± 0.0	–0.7 ± 0.0	–1.4 ± 0.0	2.5 ± 0.0
L258F	**–4.5 ± 0.0**	**–2.3 ± 0.0**	**–1.8 ± 0.0**	**–2.6 ± 0.0**	**–2.6 ± 0.0**	**–1.1 ± 0.1**
L258Y	**–4.2 ± 0.0**	**–2.2 ± 0.0**	**–0.7 ± 0.0**	**–1.7 ± 0.0**	**–2.6 ± 0.0**	**–0.7 ± 0.1**
S259P	–0.4 ± 0.0	–0.5 ± 0.0	–0.3 ± 0.0	–0.2 ± 0.0	–0.4 ± 0.0	8.4 ± 0.1
E265A	**–1.1 ± 0.3**	**–1.2 ± 0.0**	**–0.2 ± 0.0**	**–1.2 ± 0.1**	**–0.8 ± 0.0**	**–3.1 ± 0.2**
E265C	**–0.1 ± 0.0**	**–1.1 ± 0.0**	**–0.1 ± 0.0**	**–0.9 ± 0.1**	**–0.7 ± 0.0**	**–4.6 ± 0.2**
E265D	**–0.2 ± 0.0**	**–0.9 ± 0.0**	**–0.3 ± 0.0**	**–1.0 ± 0.1**	**–0.2 ± 0.0**	**–0.7 ± 0.0**
E265F	**–0.6 ± 0.3**	**–0.6 ± 0.0**	**–0.1 ± 0.0**	**–0.8 ± 0.1**	**–0.2 ± 0.0**	**–15.7 ± 0.1**
E265G	–0.4 ± 0.5	–2.7 ± 0.0	–7.5 ± 0.0	–1.5 ± 0.0	–4.5 ± 0.0	3.8 ± 0.2

E265H	**–0.2 ± 0.0**	**–0.8 ± 0.0**	**–0.1 ± 0.0**	**–1.1 ± 0.1**	**–0.2 ± 0.0**	**–8.4 ± 0.2**
E265N	**–0.2 ± 0.0**	**–1.0 ± 0.0**	**–0.1 ± 0.0**	**–1.1 ± 0.1**	**–0.4 ± 0.0**	**–4.3 ± 0.1**
E265P	**–0.8 ± 0.1**	**–2.0 ± 0.0**	**–2.0 ± 0.0**	**–1.9 ± 0.1**	**–1.4 ± 0.0**	**–1.8 ± 0.1**
E265V	**–1.2 ± 0.0**	**–0.8 ± 0.0**	**–0.3 ± 0.0**	**–0.2 ± 0.0**	**–0.3 ± 0.0**	**–8.0 ± 0.0**
E265W	**–1.0 ± 0.7**	**–0.9 ± 0.0**	**–0.1 ± 0.0**	**–1.1 ± 0.1**	**–0.6 ± 0.0**	**–3.8 ± 0.2**
E265Y	**–0.5 ± 0.0**	**–0.8 ± 0.0**	**–0.2 ± 0.0**	**–1.0 ± 0.1**	**–0.5 ± 0.0**	**–11.5 ± 0.2**
G266H	–2.8 ± 0.0	–0.1 ± 0.0	–0.9 ± 0.0	–2.9 ± 0.0	–2.4 ± 0.0	9.4 ± 0.0
G266K	–2.9 ± 0.0	–5.1 ± 0.0	–5.4 ± 0.0	–2.7 ± 0.0	–0.2 ± 0.0	10.9 ± 0.0
G266R	–4.2 ± 0.1	–5.0 ± 0.0	–3.2 ± 0.4	–2.3 ± 0.0	–3.8 ± 0.0	13.7 ± 0.0
G266W	–2.3 ± 0.0	–3.1 ± 0.0	–4.1 ± 0.0	–0.3 ± 0.0	–2.5 ± 0.0	11.2 ± 1.7
S267C	0.0 ± 0.0	–0.1 ± 0.0	–0.2 ± 0.0	–0.1 ± 0.0	0.0 ± 0.0	1.0 ± 0.0
S267I	–0.1 ± 0.0	–0.2 ± 0.0	–0.6 ± 0.0	–0.2 ± 0.0	–0.1 ± 0.0	3.3 ± 0.0
S267L	**0.0 ± 0.0**	**–0.1 ± 0.0**	**–0.5 ± 0.0**	**–0.2 ± 0.0**	**–0.1 ± 0.0**	**–1.7 ± 0.0**
S267P	–0.1 ± 0.0	–0.2 ± 0.0	–1.7 ± 0.1	–0.6 ± 0.0	–0.3 ± 0.0	10.6 ± 0.0.
S267T	**0.0 ± 0.0**	**–0.1 ± 0.0**	**–0.2 ± 0.0**	**–0.1 ± 0.0**	**–0.1 ± 0.0**	**–0.2 ± 0.0**
S267V	–0.1 ± 0.0	–0.2 ± 0.0	–0.4 ± 0.0	–0.2 ± 0.0	–0.1 ± 0.0	0.5 ± 0.0
S267W	**–2.1 ± 0.0**	**–0.6 ± 0.0**	**–2.9 ± 0.0**	**–0.2 ± 0.0**	**–1.0 ± 0.0**	**–2.0 ± 0.0**
S267Y	**–2.6 ± 0.0**	**–0.7 ± 0.0**	**–3.2 ± 0.0**	**–0.4 ± 0.0**	**–0.3 ± 0.0**	**–2.1 ± 0.0**

[a]Mean ± standard deviation

Table S2 Prediction, assessment, and visualization of potential residue pairs of disulfide bonds.

Disulfide bond	Predicted by[a]	FoldX (kcal/mol)[b]	Visual inspection	Disulfide bond	Predicted by[a]	FoldX (kcal/mol)[b]	Visual inspection
10-13	3	0.7 ± 0.2	/	241-243	1/2	–1.3 ± 0.1	Failed
100-106	1/2/3	5.3 ± 0.1	/	25-42	3	2.8 ± 0.1	/
100-108	3	5.4 ± 0.1	/	26-42	3	3.0 ± 0.0	/
103-106	1/2/3	0.8 ± 0.0	/	264-269	1/2/3	0.4 ± 0.0	/
105-184	2	3.2 ± 0.0	/	31-35	3	5.8 ± 0.1	/
106-184	1/3	0.9 ± 0.1	/	33-55	1/3	1.7 ± 0.2	/
133-134	1	1.9 ± 0.0	/	47-50	3	4.9 ± 1.4	/
134-137	1/3	4.6 ± 0.4	/	49-72	1	2.8 ± 0.0	/
138-169	1	1.9 ± 0.0	/	50-68	3	4.9 ± 0.0	/
140-171	3	2.2 ± 0.2	/	53-67	1/2	4.7 ± 0.0	/
141-155	3	5.4 ± 0.5	/	55-66	1	4.1 ± 0.0	/
160-161	1	3.6 ± 0.5	/	58-118	3	–0.8 ± 0.1	Failed
165-170	1	7.3 ± 0.1	/	58-119	3	–0.2 ± 0.2	Failed
167-193	2	5.9 ± 0.0	/	58-63	1/2	–1.7 ± 0.1	Failed
168-169	1	1.8 ± 0.0	/	61-115	1/3	–0.9 ± 0.4	Passed
172-141	3	6.5 ± 0.0	/	61-63	1	0.5 ± 1.0	/
172-155	3	1.7 ± 0.0	/	6-243	3	0.3 ± 0.1	/
172-196	1	7.7 ± 0.1	/	63-115	1	–0.1 ± 0.2	Failed
18-261	1	4.9 ± 0.0	/	64-57	3	–0.7 ± 0.2	Failed
183-217	3	4.5 ± 0.0	/	66-33	3	6.0 ± 0.0	/
188-103	3	4.6 ± 0.1	/	68-77	1	6.8 ± 0.1	/
189-219	1/2	4.8 ± 0.1	/	73-75	1	–0.1 ± 0.1	Failed
190-238	1/2/3	-3.5 ± 0.6	Passed	74-137	1	5.3 ± 0.5	/
192-194	1	4.4 ± 0.2	/	75-138	3	0.2 ± 0.0	/
199-223	3	0.3 ± 0.3	/	78-141	1	5.9 ± 0.1	/
20-173	1/2	5.7 ± 0.3	/	79-27	3	2.4 ± 0.1	/

219-190	3	2.4 ± 0.1	/	79-66	3	6.1 ± 0.0	/
220-196	3	4.7 ± 0.4	/	80-150	1/3	4.7 ± 0.0	/
22-46	3	1.6 ± 0.2	/	80-65	3	12.3 ± 1.1	/
226-231	3	2.1 ± 0.0	/	97-107	1	3.4 ± 0.1	/
227-231	1/2/3	0.5 ± 0.0	/	98-110	1/2	0.2 ± 0.0	/
228-229	2	1.3 ± 0.1	/	210-95	3	/	/
9-13	1/3	/	/	21-175	1/3	/	/
106-185	1/2	/	/	21-260	1/2	/	/
107-182	1	/	/	218-240	1/3	/	/
108-113	3	/	/	219-186	3	/	/
108-180	3	/	/	222-235	1	/	/
109-112	1/3	/	/	224-244	1/2	/	/
112-149	1/2	/	/	232-9	3	/	/
119-56	3	/	/	235-222	3	/	/
137-74	3	/	/	235-241	1/3	/	/
141-151	1/3	/	/	***235-244***	***1/2/3***	***/***	***/***
141-78	3	/	/	24-144	1/2	/	/
142-173	1/3	/	/	243-235	3	/	/
142-24	3	/	/	244-224	3	/	/
142-79	3	/	/	252-205	3	/	/
143-147	3	/	/	256-203	3	/	/
144-145	1	/	/	256-253	3	/	/
144-147	3	/	/	260-175	3	/	/
144-176	3	/	/	260-21	3	/	/
147-81	3	/	/	260-265	3	/	/
148-174	3	/	/	261-18	3	/	/
148-177	3	/	/	26-43	3	/	/
149-112	3	/	/	265-144	3	/	/
151-143	3	/	/	27-81	1/3	/	/
151-174	3	/	/	***29-268***	***1/2/3***	***/***	***/***

174-177	2/3	/	/	29-32	1	/	/
175-144	3	/	/	29-40	3	/	/
175-199	1/3	/	/	32-29	3	/	/
176-145	3	/	/	38-50	3	/	/
179-216	1/2	/	/	***40-43***	***1/2/3***	**/**	**/**
179-218	3	/	/	43-38	3	/	/
180-149	3	/	/	43-44	1	/	/
181-108	3	/	/	47-70	3	/	/
182-107	3	/	/	56-122	1/2/3	/	/
184-105	3	/	/	62-83	1	/	/
185-106	3	/	/	63-58	3	/	/
185-181	3	/	/	66-55	3	/	/
186-217	1	/	/	70-73	1/2/3	/	/
186-219	1	/	/	70-75	3	/	/
196-172	3	/	/	72-49	3	/	/
198-220	3	/	/	80-143	2/3	/	/
200-207	1/3	/	/	80-147	2/3	/	/
201-225	1/2	/	/	81-64	3	/	/
201-260	3	/	/	82-146	3	/	/
20-142	3	/	/	83-89	3	/	/
202-203	1	/	/	85-88	1/3	/	/
202-256	1	/	/	9-232	1/2	/	/
203-253	1	/	/	9-234	3	/	/
204-256	1/2	/	/	95-210	1	/	/
204-257	1/3	/	/	96-110	3	/	/
210-216	1/3	/	/				

[a] 1, MODIP; 2, DbD2; 3, BridgeD

[b]Mean ± standard deviation

Natural disulfide bonds are shown in bold italics.

Table S3 Quantitative detection of disulfide bonds

Sample	Free thiol/protein(mol/mol)[a]		Total number of free cysteines	Deduced number of disulfide bonds
	–DTT	+DTT		
WT	0.1 ± 0.1	6.2 ± 0.6	0	3
E265V/S267W	0.0 ± 0.1	5.9 ± 0.3	0	3
E265V/S267W/S61C-S115C	0.1 ± 0.1	8.2 ± 0.3	0	4
E265V/S267W/E190C-E238C	0.0 ± 0.1	7.8 ± 0.3	0	4
M6	0.1 ± 0.1	9.8 ± 0.6	0	5

[a]Mean ± standard deviation

Table S4 Specific activity of WT and mutant ROL in measuring enzymatic properties

		Specific activity (U/mg)[a]		
		WT	**E265V/S267W**	**M6**
Optimum T	25 °C	52.0 ±1.4	112.7 ±3.6	87.2 ±3.0
	30 °C	69.7 ±2.5	171.9 ±7.1	136.4 ±5.2
	35 °C	97.5 ±3.6	202.1 ±10.1	179.9 ±6.8
	40 °C	66.1 ±1.6	156.4 ±8.6	229.1 ±3.5
	45 °C	33.1 ±1.0	85.5 ±2.4	252.2 ±9.4
	50 °C	16.5 ±0.5	52.5 ±1.4	215.7 ±7.0
Optimum pH	Phosphate buffer (7.0)	36.3±1.7	79.2±3.3	86.2±3.2
	Phosphate buffer (7.5)	56.6±2.4	121.1±5.5	134.2±3.4
	Phosphate buffer (8.0)	93.0±3.8	188.4±9.0	166.2 ± 4.1
	Tris-HCl buffer (8.0)	97.5 ± 3.5	202.1 ± 9.4	179.9 ± 6.1
	Tris-HCl buffer (8.5)	81.9 ± 3.7	169.3 ± 8.0	197.2 ± 8.4
	Tris-HCl buffer (9.0)	72.0 ± 2.9	145.7 ± 2.6	182.8 ± 7.7
	Glycine-NaOH buffer (9.0)	68.2 ± 1.4	150.3 ± 2.4	170.0 ± 2.9
	Glycine-NaOH buffer (9.05)	45.2 ± 2.6	114.0 ± 5.8	146.0 ± 6.3

[a]Mean ± standard deviation

Table S5 Studies on the activity and/or thermostability of fungal lipases

Organism	Variant(s)	Strategy	Modification		Reference
			Thermostability	Catalytic activity	
Aspergillus oryzae	V269D	Structure-guided rational design	same T_{opt}	6-fold increase in activity	Lan et al., 2021
Rhizopus chinensis	Disulfide variant	Rational design	same T_{opt}	Altered specificity	Yu et al., 2012
Rhizopus chinensis	S4-3	Rational design	2 °C increase in T_{opt}	Similar activity	Yu et al., 2012
Yarrowia lipolytica	V213P	MD simulations	5 °C increase in T_{opt}	Same activity (876.5 U/mg)	Zhang et al., 2019
Rhizomucor miehei	T18K/T22I/E230I/S56C-N63C/V189C-D238	Rosetta ddg_monomer MODIP, DbD, SSBOND, BridgeD	15 °C increase in T_{opt}	0.4-fold increase in activity	Li et al., 2018
Rhizopus oryzae	V209L/D262G/E190C/E238C	Multiple sequence alignment Disulfide bond design	15 °C increase in T_{opt}	-	Zhao et al., 2018
Rhizopus oryzae	P210F/L258F	Multiple alignment	10–20 °C decrease in T_{opt}	6.2-fold increase in activity	Ding et al., 2019
Rhizopus oryzae	E190V	Error-prone PCR DNA shuffling	10 °C increase in T_{opt}	75% of the WT in activity	Niu et al., 2006
Rhizopus oryzae	E265V/S267W/S61C-S115C/E190C-E238C	This study	10 °C increase in T_{opt}	(1.5–3.8)-fold increase in activity	This study

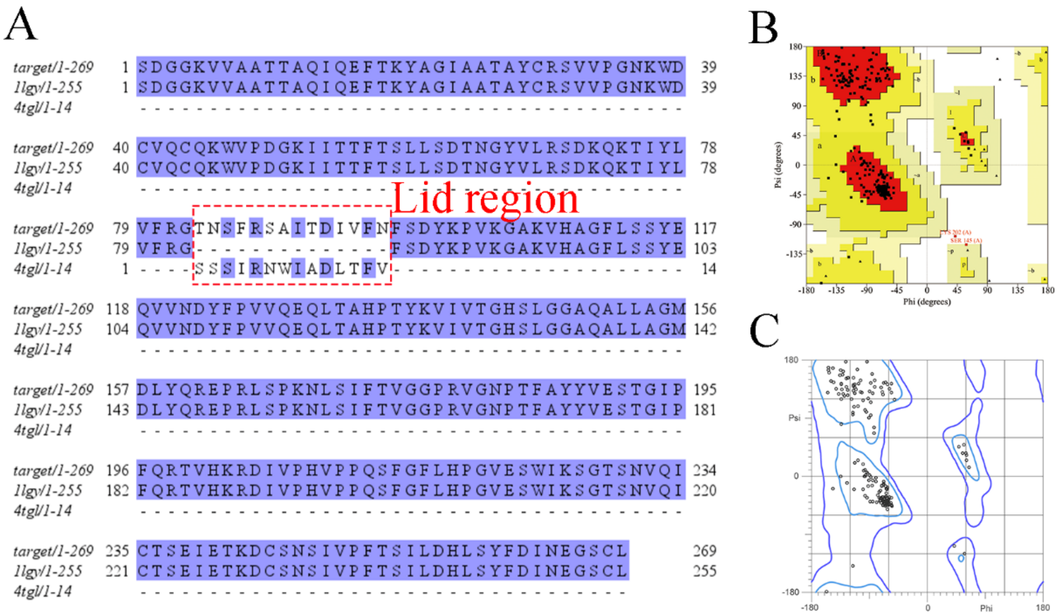

Fig. S1 Model and evaluation of ROL in open conformation (OROL). (A) Multiple sequence alignments of target sequence, lid region of RML in open conformation (PDB ID: 4tgl, residues 82–95) and closed conformation of ROL without lid region (PDB ID: 1lgy, residues 1–82 and 97–269). The alignments were conducted using the PROMALS3D server and visualized using Jalview, with coloring based on the percentage identity. Ramachandran plot analysis of targeted OROL from (B) MolProbity and (C) PROCHECK.

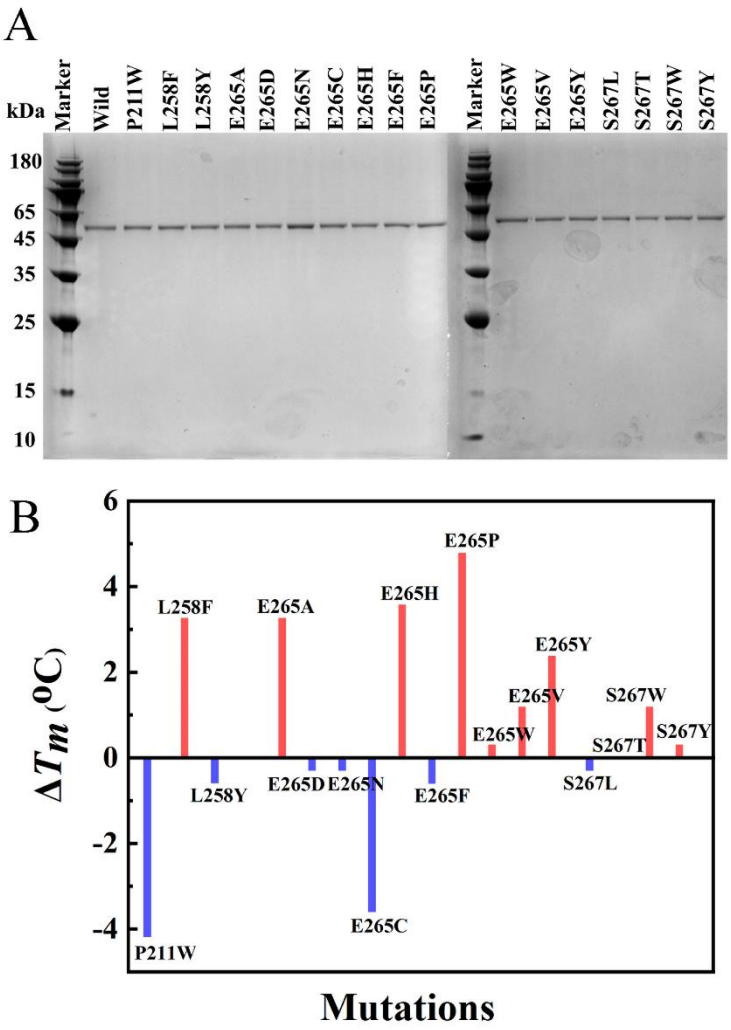

Fig. S2 (A) SDS-PAGE image of purified variants based on Cartesian_ddg using 12% separation gel and 5% stacking gel. (B) Melting temperature changes (ΔT_m) of purified variants based on Cartesian_ddg measured by differential scanning fluorimetry. The red bar represents stable candidates with positive ΔT_m value and the blue one represents unstable candidates with negative ΔT_m value.

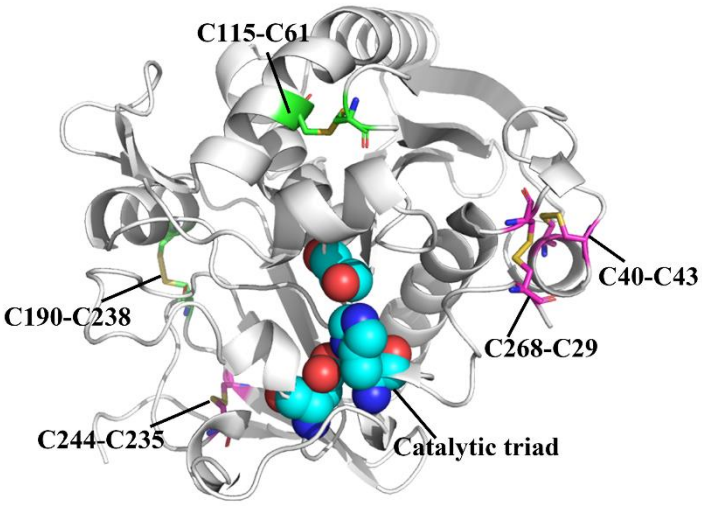

Fig. S3 Presentation of disulfide bonds of mutant M6 with the catalytic triad as spheres in cyan. The designed disulfide bonds were as sticks in green and the native disulfide bonds were as sticks in magenta.

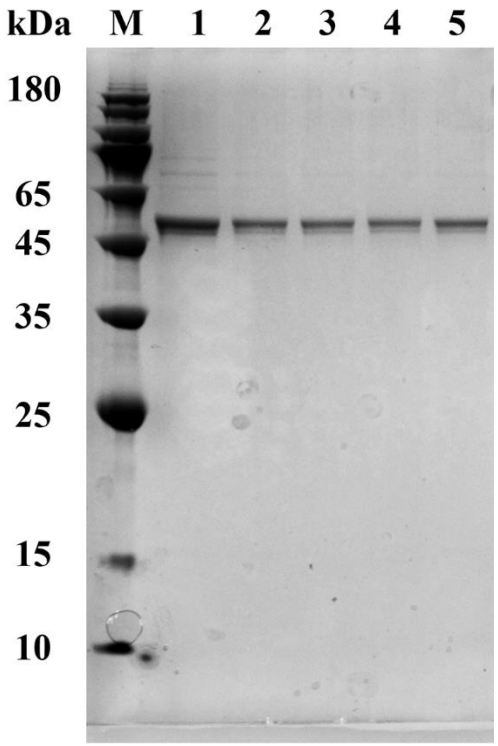

Fig. S4 SDS-PAGE image of disulfide bond mutants using 12% separation gel and 5% stacking gel. (M: marker; 1: WT; 2: E265V/S267W; 3: E265V/S267W/E190C-E238C; 4: E265V/S267W/S61C-S115C; 5: M6).

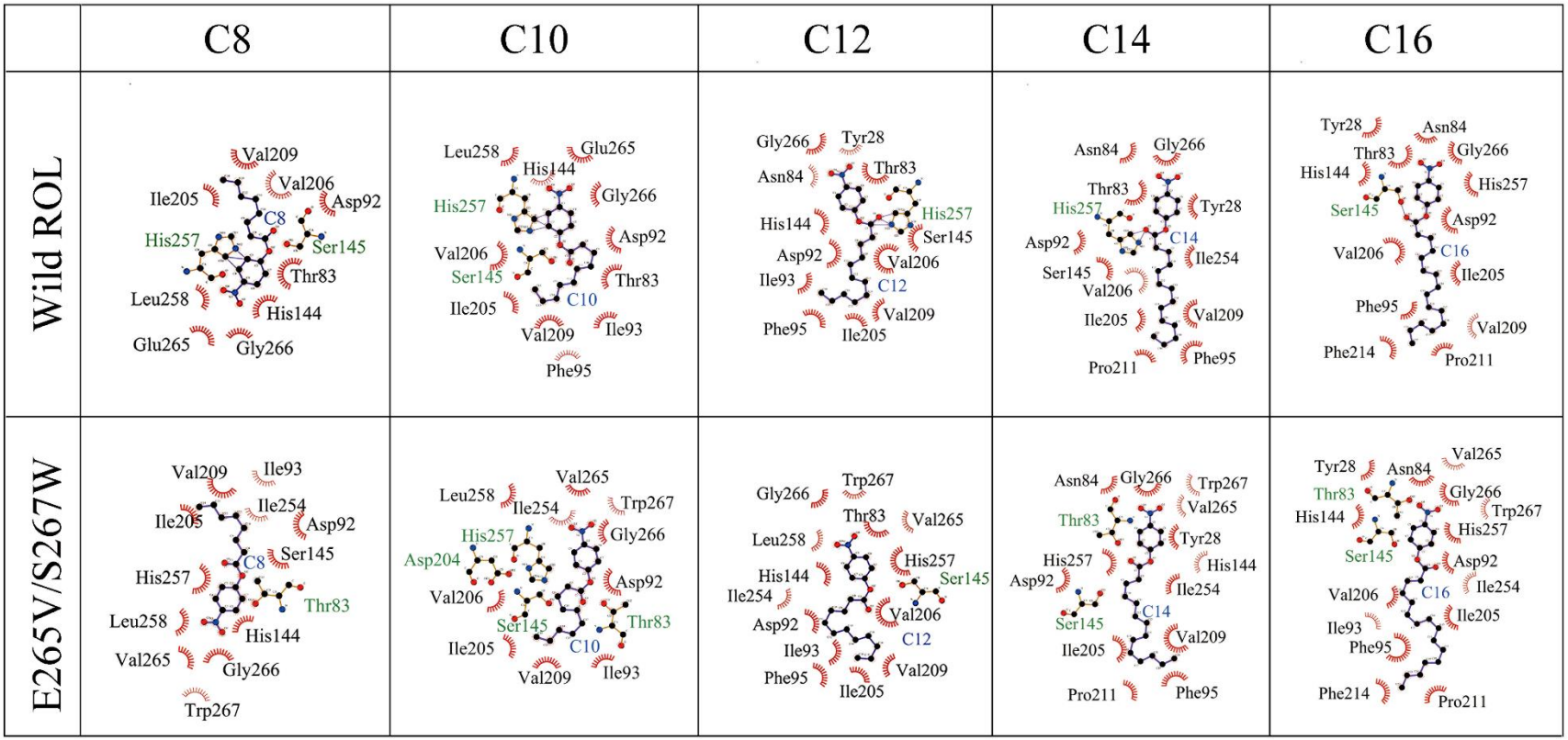

Fig. S5 2D diagrams of enzyme–substrate interactions of five bound ligands generated by LigPlot+, and plot of variant E265V/S267W automatically fitted to WT. The ligands are: C8, C10, C12, C14, and C16. The spoked arcs represent residues making nonbonded contacts with the ligand.

References

Ding X, Tang XL, Zheng RC, Zheng YG. 2019. Identification and engineering of the key residues at the crevice-like binding site of lipases responsible for activity and substrate specificity. Biotechnol Lett 41:137-146.

Lan DM, Zhao G, Holzmann N, Yuan SG, Wang J, Wang YH. 2021. Structure-guided rational design of a mono- and diacylglycerol lipase from *Aspergillus oryzae*: a single residue mutant increases the hydrolysis ability. J Agric Food Chem 69:5344-5352.

Li GL, Fang XR, Su F, Chen Y, Xu L, Yan YJ. 2018. Enhancing the thermostability of *Rhizomucor miehei* lipase with a limited screening library by rational-design point mutations and disulfide bonds. Appl Environ Microbiol 84:e02129-17.

Niu WN, Li ZP, Zhang DW, Yu MR, Tan TW. 2006. Improved thermostability and the optimum temperature of *Rhizopus arrhizus* lipase by directed evolution. J Mol Catal B Enzym 43:33-39.

Yu XW, Tan NJ, Xiao R, Xu Y. 2012. Engineering a disulfide bond in the lid hinge region of *Rhizopus chinensis* lipase: increased thermostability and altered acyl chain length specificity. PLoS One 7:e46388.

Yu XW, Wang R, Zhang M, Xu Y, Xiao R. 2012. Enhanced thermostability of a *Rhizopus chinensis* lipase by in vivo recombination in *Pichia pastoris*. Microb Cell Fact 11:102.

Zhang HT, Sang JC, Zhang Y, Sun TW, Liu H, Yue R, Zhang J, Wang HK, Dai YJ, Lu FJ, Liu FF. 2019. Rational design of a *Yarrowia lipolytica* derived lipase for improved thermostability. Int J Biol Macromol 137:1190-1198.

Zhao JF, Wang Z, Gao FL, Lin JP, Yang LR, Wu MB. 2018. Enhancing the thermostability of *Rhizopus oryzae* lipase by combined mutation of hot-spots

and engineering a disulfide bond. RSC Adv 8:41247-41254.